Erschienen in: Solar Energy Materials and Solar Cells ; 72 (2002), 1-4. - S. 453-464
https://dx.doi.org/10.1016/S0927-0248(01)00193-3

Current collecting channels in RGS silicon solar cells—are they useful?

G. Hahn[a,*], D. Sontag[a], C. Haessler[b]

[a] *Department of Physics, University of Konstanz, P.O.Box X916, 78457 Konstanz, Germany*
[b] *Bayer AG, Rheinuferstr. 7-9, 47812 Krefeld, Germany*

Abstract

Ribbon growth on substrate (RGS) silicon could be the crystalline silicon material for PV of the future. The extremely fast production technique avoiding any material losses due to sawing drastically reduces the wafering costs. On the other hand, one has to deal with more crystal defects (grain boundaries, dislocations, impurities), which especially limit the diffusion length and normally result in small short-circuit current densities J_{sc}. The charge carrier collection probability can be increased by a macroscopic V-texture of the surface, but even more effective would be a 3-dimensional emitter structure within the whole bulk cell volume. This was observed in some RGS solar cells showing minority carrier lifetimes of only around 0.4 μs after cell processing, but J_{sc} of above 34 mA/cm^2. In these cells, the whole bulk volume collects current despite the small diffusion lengths. This behaviour was investigated using spatially resolved lifetime and internal quantum efficiency mappings, capacitance measurements and a special EBIC technique, where the electron beam hits the backside of the wedge-shaped solar cell. From our results, we conclude that the collecting structures may be caused by inversion in combination with a high O content. Cells with large areas of collecting channels exhibit lower fill factors, but nearly no loss in open-circuit voltage as compared to the standard RGS cells. For both types of cells, confirmed record efficiencies of 12.5% have been obtained.

Keywords: RGS; Ribbon; Texture; Diffusion length; Lifetime; Carrier collecting channels

1. Introduction

Ribbon growth on substrate (RGS) silicon was developed by Bayer and is still in the R&D phase [1]. As it is a ribbon technique, it makes use of all advantages linked

*Corresponding author. Tel.: +49-7531-88-3644; fax: +49-7531-88-3895.
E-mail address: giso.hahn@uni-konstanz.de (G. Hahn).

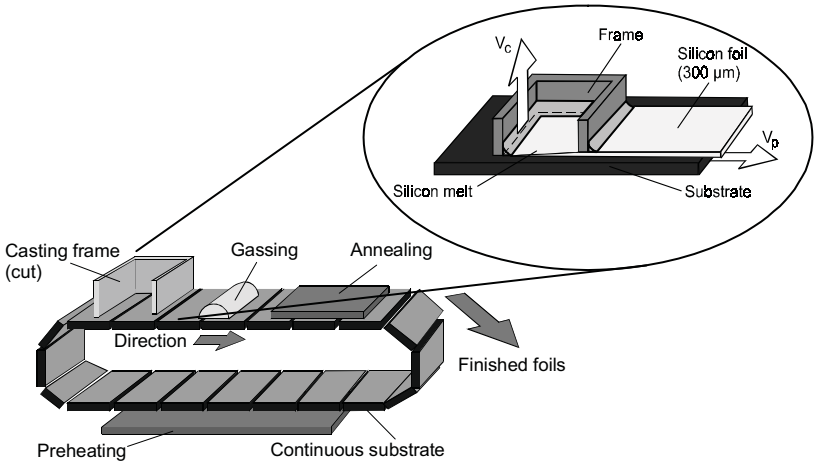

Fig. 1. Schematic diagram of the continuous RGS technique using substrates on a conveyor belt.

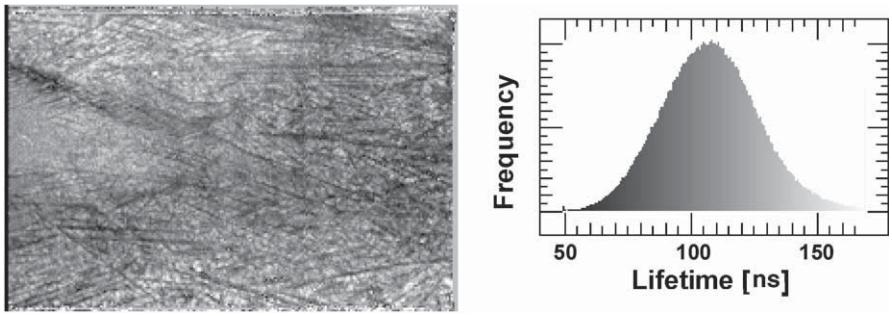

Fig. 2. µ-PCD lifetime map of an as-grown RGS wafer ($8 \times 12\,cm^2$).

to these techniques: No material losses due to sawing of the ingot and wafers as well as less energy consumption. A main difference between other techniques already commercialised (e.g. edge-defined film-fed growth from ASE) is the very fast production of around 1 wafer/s due to the decoupling of direction of pulling and crystallisation. Fig. 1 shows the schematic principle of the RGS technique foreseen in the future. A conveyor belt transports the substrates on which the $\sim 300\,\mu m$ thick wafers crystallise. The wafers leave the substrate and can be used for cell processing.

This extremely fast technique obtains a significant reduction in wafering costs. The material used for this study was produced in a lab-scale machine which did not run in a continuous mode. Due to the high concentration of crystal defects and high oxygen as well as carbon content, as-grown bulk lifetimes τ_b are $\approx 0.1\,\mu s$ (Fig. 2). All solar cells for this study have been processed completely at the University of

Konstanz. After cell processing without bulk passivation steps, the diffusion length L_{diff} is typically below 20 μm and limits the short-circuit current density J_{sc}.

2. Enhancing J_{sc}

2.1. H-passivation

Defects can be passivated and cell parameters increased by the incorporation of hydrogen in the silicon bulk. This is normally done within the cell process via a hydrogen-rich SiN_x layer and a subsequent firing step to release the hydrogen into the bulk. In our study, we used microwave-induced remote hydrogen plasma passivation [2], which turned out to be very effective in former studies [3–5]. Using this technique, τ_{b} increases to $0.4 < \tau_{\mathrm{b}} < 0.6\,\mu\mathrm{s}$, corresponding to $L_{\mathrm{diff}} < 40\,\mu\mathrm{m}$ after cell processing.

2.2. Macroscopic V-texture

J_{sc} of multicrystalline silicon solar cells can be improved by a V-texture of the front surface. A macroscopic mechanical texture using a conventional wafer-dicing saw is beneficial for materials showing small diffusion lengths in a threefold way: The light has several chances to enter the cell, resulting in a lesser reflection; electron-hole pairs are created nearer to the surface due to the inclined penetration of the light; collection probability increases because of the reduced distance to the collecting surface emitter (Fig. 3). We could experimentally prove that by applying a

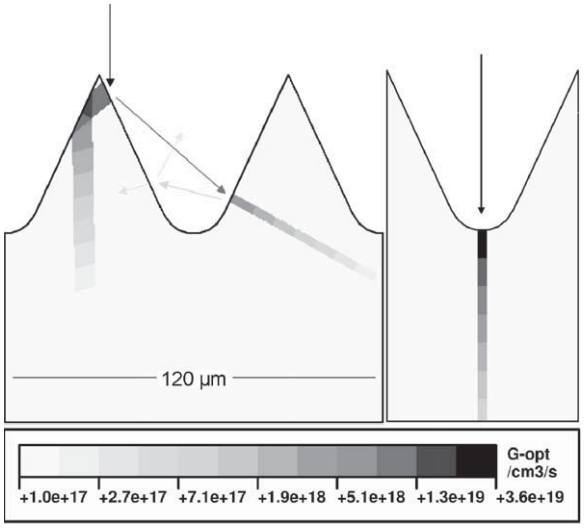

Fig. 3. Geometry of a V-textured cell surface and profiles of generated charge carriers.

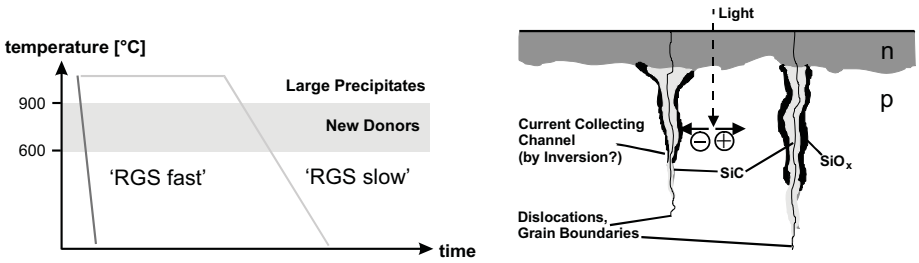

Fig. 4. Left: RGS cooling sequences after crystallisation. For this study, the 'RGS slow' process was chosen. Right: Proposed model for current-collecting channels based on SiC and SiO_x at extended defects.

mechanical V-texture to RGS solar cells, an increase in efficiency η of 7–8%$_{rel}$ depending on L_{diff} is possible [6].

2.3. 3-dimensional emitter structure

Even more effective for materials with small L_{diff} would be a 3-dimensional emitter structure not only on the surface but also within the bulk of the cell. Carrier collection would be nearly independent of L_{diff}, supposing the spacing between the emitter structures is $< L_{diff}$.

Bayer AG developed a special cooling sequence directly after crystallisation in order to cope with the high interstitial oxygen concentration. During an annealing step above 900°C large oxygen precipitates are formed to prevent the formation of new donors at high temperature steps in the subsequent cell process [7] (Fig. 4). In the former experiments, we could observe that large precipitates are less detrimental concerning the reduction of L_{diff} in the solar cell as compared to the formation of new donors during high temperature steps in the standard solar cell processing without an initial annealing step (see also Ref. [8]). In the last few years, unusually high values for J_{sc} have been reported for RGS solar cells. A model proposed by Haessler et al. [8] suggested that the precipitation of oxygen and/or carbon at extended defects could lead to a 3-dimensional current-collecting structure, caused by inversion [9]. In the next section, we will try to supply evidence for the existence of these current-collecting channels.

3. Carrier-collecting channels

3.1. IQE measurement

In some parts of RGS solar cells, IQE values close to unity can be observed at a wavelength of 905 nm (penetration depth 32 μm). This leads to J_{sc} values above 30 mA/cm^2 despite comparably low lifetimes $\tau_b < 0.6$ μs. In Fig. 5, the spatially

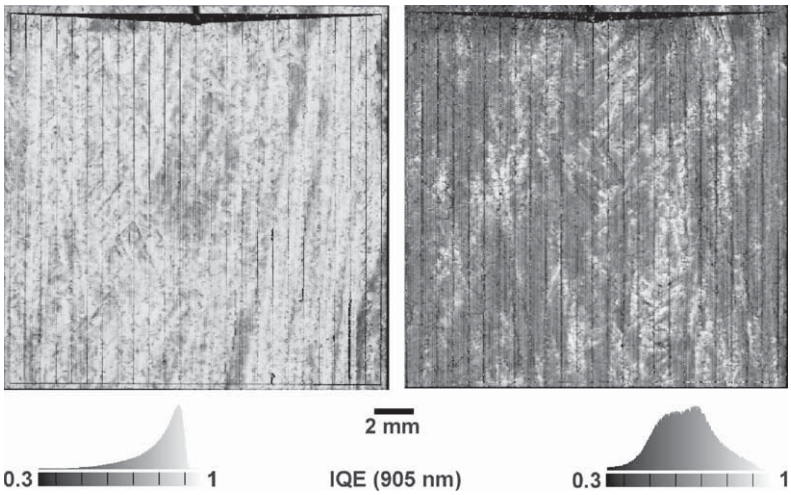

Fig. 5. IQE at 905 nm of two RGS solar cells with exceptionally high J_{sc} of 34.5 mA/cm^2 (left) and of rather moderate J_{sc} of 31.1 mA/cm^2, respectively (right). In both cells, τ_b is $<0.6\,\mu s$.

resolved IQE at 905 nm of two RGS cells originating from the same batch process can be seen. Cell 1 shows very high IQEs in most parts of the wafer leading to an outstanding J_{sc} of 34.5 mA/cm^2, despite a lifetime value $\tau_b < 0.6\,\mu s$. Within cell 2 only a minor part shows high IQEs leading to a broader distribution in the histogram and J_{sc} of 31.1 mA/cm^2. Such high currents exceeding 30 mA/cm^2 combined with low lifetimes cannot be explained assuming a conventional planar emitter structure close to the wafer surface.

3.2. Minority charge carrier mobilities

The diffusion constant of minority charge carriers D_n (for p-type material) is an important characteristic for the electronic behaviour of the solar cell. Recently, we developed a method to derive a map of D_n which is proportional to the minority charge carrier mobility μ_n via

$$\mu_n = \frac{k_B T}{q} D_n. \tag{1}$$

We measured the spatially resolved IQE at three wavelengths (833, 905, and 980 nm) and calculated the effective diffusion length L_{eff} according to the method proposed by Basore [10]. For small diffusion lengths as in RGS, L_{eff} can be equated with L_{diff}. After removing the metal contacts, we mapped τ_b using microwave-detected photoconductance decay (μ-PCD). With

$$L_{diff} = \sqrt{D_n \tau_b}, \tag{2}$$

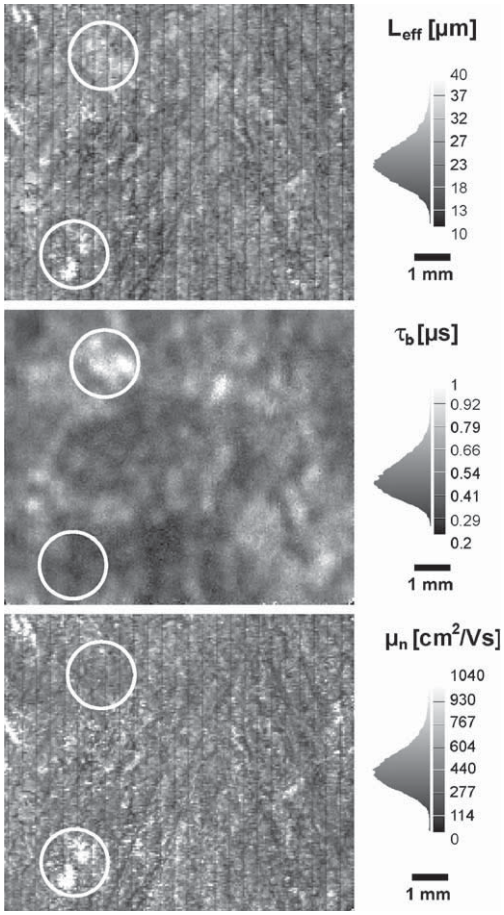

Fig. 6. Determination of minority charge carrier mobility μ_n (bottom) for an RGS solar cell using L_{diff} from IQE (top) and τ_b from µ-PCD measurements (middle).

a map of D_n or μ_n using Eq. (1) could be obtained. A more detailed description can be found in Ref. [11]. The resulting maps of L_{diff}, τ_b and μ_n are given in Fig. 6. In most regions, a high L_{diff} is linked with a high τ_b leading to the average values of μ_n (e.g. upper circle). But for some areas with apparently high L_{diff} and only moderate or even low τ_b the values for μ_n are above 1240 cm^2/Vs, which is the value expected for monocrystalline silicon of the same resistivity (lower circle) [12]. These anomaly high values for RGS, where mobilities are expected to be a factor 2–3 lower than in monocrystalline silicon [13], show that within these regions, L_{diff} could not be properly determined using the fit algorithm suggested in [10]. A non-planar emitter structure would lead to higher values for L_{diff} in these parts of the cell, and therefore, mobilities $> 1240\,cm^2/Vs$ according to Eqs. (1) and (2) indicate the regions with 3-dimensional current collection in the bulk.

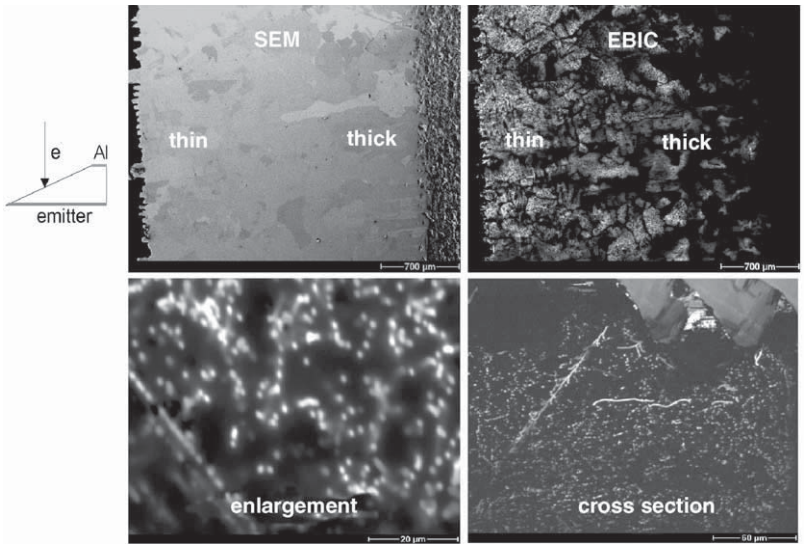

Fig. 7. EBIC investigation of a V-textured RGS solar cell showing an exceptionally high IQE. Top left: SEM picture of the wedge-shaped cell from the back. Top right: EBIC image of the same area. Even in thick areas close to the Al back contact, an efficient current collection is visible. Bottom left: Close-up of the previous picture resolving individual point-like channels. Bottom right: Cross-section of the cell revealing the V-texture and the collecting channels within the whole bulk volume of the cell. (EBIC analysis carried out by M. Langenkamp, MPI Halle, Germany).

3.3. EBIC analysis

A special EBIC set-up was used to detect the current-collecting structure microscopically. The cell's backside was ground wedge-shaped and the electron beam hit the cell from the backside. Results can be seen in Fig. 7. Even in some thick areas ($>200\,\mu m$), a good EBIC contrast is visible. The enlarged picture reveals single 'point-like' structures leading the current from the backside to the front-side emitter. These defects can be correlated to etch pits at emerging dislocations [9]. Therefore, we conclude that in regions with good EBIC contrast, extended defects like dislocations and grain boundaries form a 3-dimensional current-collecting network which is linked to the front-side emitter. In this way, the whole silicon bulk collects current because the spacing between the channels is $<L_{\mathrm{diff}}$ as can be seen in the cross-section picture of Fig. 7.

3.4. TEM study

Transmission electron microscopy (TEM) was used to detect the nature of the current collecting structures. Therefore, samples from two cell regions have been prepared of which one shows a high IQE, while the other shows a normally low IQE. Two typical pictures obtained from this study are presented in Fig. 8. Dislocations in

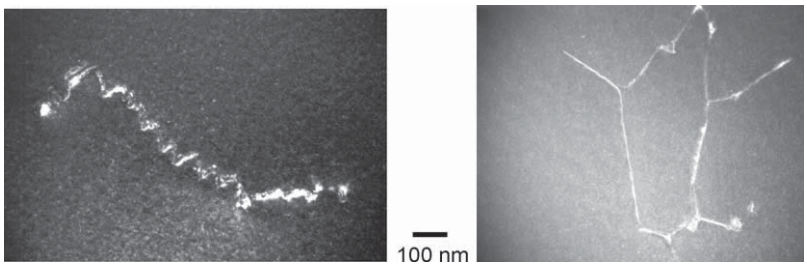

Fig. 8. Representative dislocations from two areas within RGS solar cells. In an area of high IQE, dislocations are heavily decorated with precipitates forming a continuous line (left). In the area of low IQE, dislocations are not continuously decorated with precipitates (right). (TEM investigation carried out by M. Werner, MPI Halle, Germany).

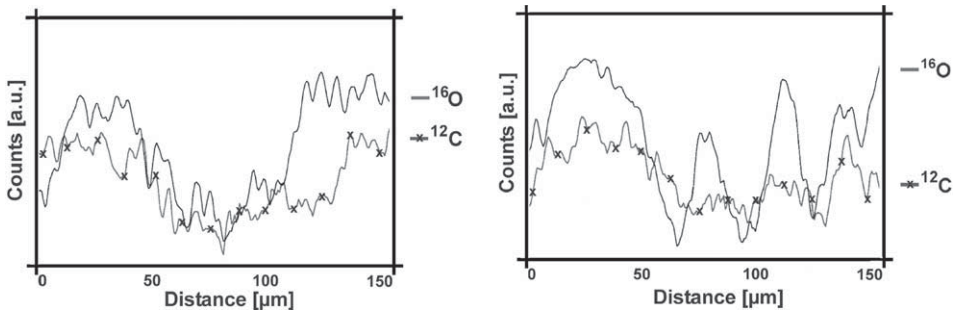

Fig. 9. Spatially resolved SIMS measurements (linescans) of an RGS solar cell. In the area with high IQE, sharp ^{16}O peaks with spacing $<10\,\mu m$ are visible (left). The area with low IQE does not show this substructure within the ^{16}O concentration (right).

the high IQE region are all heavily decorated with precipitates, whereas the low IQE area shows less precipitation at dislocations (although some precipitates are visible). Closely packed precipitates seem to be the reason for activating the current collection phenomenon. The precipitates are most likely related to oxygen which was in fact intentionally precipitated during the annealing step directly after crystallisation.

3.5. Spatially resolved SIMS

Spatially resolved secondary ion mass spectroscopy (SIMS) was used to clarify the chemical nature of the channels. The method has a lateral resolution of 1 μm and the concentrations of C and O have been determined within a circle of 150 μm diameter in two regions of the same cell exhibiting a high and low IQE, respectively. Linescans through both these circles are given in Fig. 9. The drop of concentration towards the centre visible in both regions for both elements is caused by the apparatus and can be neglected. There seems to be no difference in the behaviour of the C concentration

showing narrow peaks in both areas. But for the oxygen concentration, narrow peaks indicating a high local concentration[1] can only be seen in the high IQE region, whereas in the low IQE region, only broader peaks without a distinct substructure can be detected. As the SIMS resolution is 1 μm and the expected spacing of the channels is in the range of 5–10 μm (Fig. 7), we assume that oxygen precipitation at dislocations is the cause for the current collection phenomenon. This is the first experimental evidence of the chemical nature of the collecting channels.

3.6. Capacitance measurements

Capacitance measurements at high (100 kHz, C_{HF}) and low (100 Hz, C_{LF}) frequencies have been carried out at Bayer for a complete set of RGS cells processed in one batch. The cells are mechanically V-textured and do not have an antireflective coating. Some cells show different capacities dependent on the frequency used for the measurement. In all cases, capacities at low frequency are larger than those at high frequency. A difference in both capacities indicates a slow charge-carrier exchange that contributes only to C_{LF} and is typical for minority charge carriers being involved [8]. The explanation given in a former study [8] was that the change of conduction type of the channels is not due to a change in doping concentration, but results from inversion which can be caused by the closely packed oxygen precipitates at dislocations detected in this study using different characterisation methods. The physical model is presented in more detail in Ref. [9].

In Fig. 10, the relation between cell parameters and the difference in low- and high-frequency capacity $\Delta C(C_{LF} - C_{HF})$ is given. Obviously, currents densities above 25 mA/cm^2 (V-textured cells, no antireflective coating) can only be obtained by using the current-collecting channels ($\Delta C > 0$). More channels lead to a larger J_{sc} and correspond to an increase in ΔC.

4. Discussion

The answer to the question whether collecting channels are useful or not must be given based on the cell efficiency level. Therefore, the results of the capacitance measurements shown in Fig. 10 provide the kind of information we are interested in. Assuming that ΔC supplies a measure of the amount of channels located in the cell, we can begin to discuss their influence on the cell parameters. Only tendencies will be addressed taking into account the best cells for each particular concentration of channels, indicated by the lines drawn in Fig. 10. High values of J_{sc} can only be reached using a certain amount of channels. For V_{oc}, only a loss of around 10 mV can be detected for the best cells, which is mainly caused by a poor second diode suffering from recombination in the multiply enlarged space-charge region. The poor second diode is more detrimental to the fill factor behaviour. A clear tendency towards lower fill factors can be observed for increasing ΔC. Additionally, shunting

[1] Concentration could be even higher if the resolution is <1 μm.

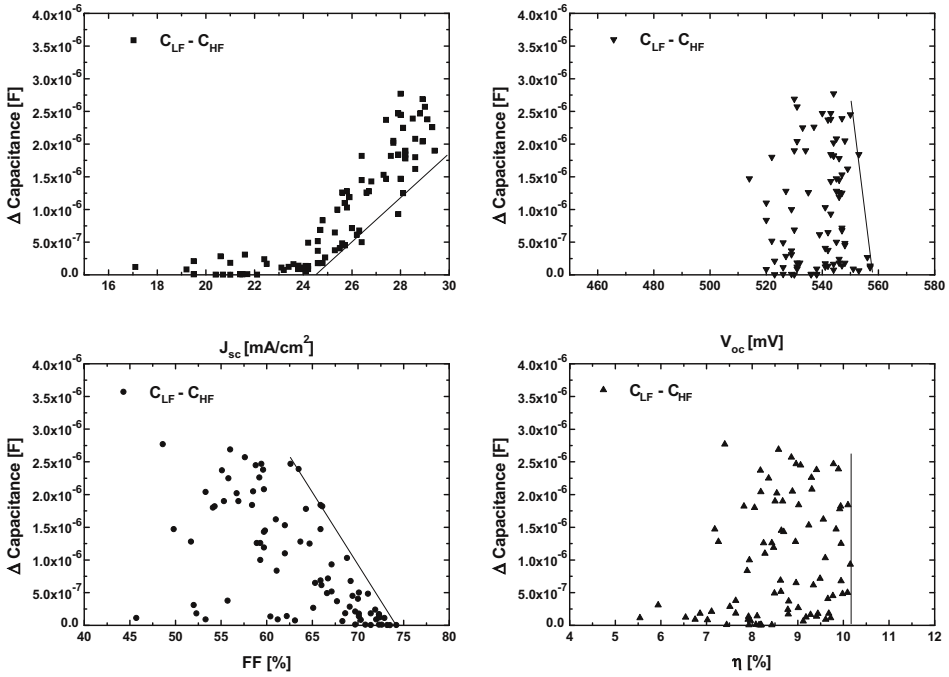

Fig. 10. Capacitance measurements for a set of RGS solar cells (4 cm^2, V-textured surface, no antireflective coating). The difference between the signal at low frequency (100 Hz, C_{LF}) and high frequency (100 kHz, C_{HF}) dependent on the solar cell parameters is shown. The lines serve as a guide to the eye.

problems may have an influence. For the maximum efficiency, no negative effect caused by the channels can be detected, as efficiencies around 10% (without antireflective coating) can be reached almost independently on ΔC. After a ZnS/MgF_2 antireflective coating confirmed record efficiencies of 12.5% have been obtained on cells containing a high (34.5 mA/cm^2, 549 mV, 65.9% FF) and low (31.1 mA/cm^2, 560 mV, 71.6% FF) amount of collecting channels (cell area 4 cm^2). Cells with current-collecting channels may lead to higher efficiencies in the future if fill factor problems could be solved by an even better passivation.

Currently, a new continuously operating RGS production machine is built, that works in thermal equilibrium, which was not the case for the lab-type machine used for the material investigated in this study. For the new machine, a lower oxygen and impurity concentration in the produced wafer is expected, which might lead to higher starting lifetimes and diffusion lengths in the processed solar cells and higher J_{sc}s without using the channels. Until this is proven, carrier-collecting channels remain an elegant tool to use in the whole bulk volume of a silicon material with small L_{diff} for carrier collection and therefore an enhancement of J_{sc} within a solar cell.

5. Summary

RGS silicon has the potential to drastically reduce the wafering costs due to a very fast production of the ribbons. A higher defect density as compared to other materials currently limits τ_b to values $<0.6\,\mu s$ in finished solar cell structures. A macroscopic mechanical V-texture of the surface leads to higher currents and efficiencies due to a higher collection probability. Some cells have shown unusually high values of IQE and J_{sc} which cannot be explained with a planar emitter structure at the cell surface (mobility measurement). This 3-dimensional carrier collecting structure is linked to extended crystal defects like dislocations as could be visualised by EBIC investigations. TEM analysis revealed closely packed precipitates at dislocations in areas of high IQE and spatially resolved SIMS measurements suggest to identify them as oxygen related. Capacitance measurements in dependency on the frequency demonstrate a connection between increasing J_{sc} and a large difference between low and high frequency capacitance signals. From all these results, we conclude that the high currents are caused by closely packed oxygen-related precipitates at extended defects (e.g. dislocations) and conduction by locally inversion of the p-type material at these structures. For cells with both, very high concentration of channels as well as only moderate concentration, record efficiencies of 12.5% have been reached. Therefore, there seems to be no detrimental effect of the channels concerning η_{max}. A new RGS production machine will probably fabricate wafers with lower impurity concentration, and therefore higher lifetimes in the processed solar cells might make additionally current collection by channels unnecessary.

Acknowledgements

We like to thank M. Keil for assistance during solar cell processing and Bayer AG for the financial support for SIMS measurements. This work was partly financed by the German BMWi within the KoSi project (0329858J).

References

[1] H. Lange, I.A. Schwirtlich, J. Cryst. Growth 104 (1990) 108.
[2] M. Spiegel, P. Fath, K. Peter, B. Buck, G. Willeke, E. Bucher, Proceedings of the 13th EC PVSEC, Nice, 1995, p. 421.
[3] M. Spiegel, G. Hahn, W. Jooss, S. Keller, P. Fath, G. Willeke, E. Bucher, Proceedings of the Second WC PVSEC, Vienna, 1998, p. 1685.
[4] G. Hahn, W. Jooss, M. Spiegel, P. Fath, G. Willeke, E. Bucher, Proceedings of the 26th IEEE PVSC, Anaheim, 1997, p. 75.
[5] G. Hahn, C. Zechner, M. Spiegel, W. Jooss, P. Fath, G. Willeke, E. Bucher, Proceedings of the Second WC PVSEC, Vienna, 1998, p. 1840.
[6] G. Hahn, C. Zechner, M. Rinio, P. Fath, G. Willeke, E. Bucher, J. Appl. Phys. 86 (12) (1999) 7179.
[7] W. Koch, H.-U. Hoefs, C. Haessler, S. Thurm, Proceedings of the Second WC PVSEC, Vienna, 1998, p. 1254.

[8] C. Haessler, H.-U. Hoefs, S. Thurm, O. Breitenstein, M. Langenkamp, Proceedings of the 16th EC PVSEC, Glasgow, 2000, p. 1352.
[9] O. Breitenstein, M. Langenkamp, J.P. Rakotoniaina, Solid State Phenom. 78–79 (2001) 29.
[10] P.A. Basore, IEEE Trans. Electron Devices ED-37 (1990) 337.
[11] D. Sontag, G. Hahn, P. Fath, E. Bucher, E-MRS 2001 Spring Meeting, Strasbourg 2001, Sol. En. Mater. Sol. Cells, this issue.
[12] A.B. Sproul, M.A. Green, A.W. Stephens, J. Appl. Phys. 72 (9) (1992) 4161.
[13] G. Hahn, P. Geiger, P. Fath, E. Bucher, Proceedings of the 28th IEEE PVSC, Anchorage, 2000.